A Sleeve-Based, Micromotion Avoiding, Retractable and Tear-Opening (SMART) Insertion Tool for Cochlear Implantation

Philipp Aebischer, Stefan Weder, Georgios Mantokoudis, Mattheus Vischer, Marco Caversaccio, and Wilhelm Wimmer

***Abstract*—*Objective:* In conventional cochlear implantation, the insertion of the electrode array is strongly affected by the local anatomy and human kinematics. Herein, we present a concept for an insertion tool that allows to optimize the insertion trajectory beyond anatomical constraints and stabilizes the electrode array in manual implantation. A novel sleeve-based design allows the instrument to be compliant and potentially protective to intracochlear structures, while a tear-open mechanism allows it to be removed after insertion by simply retracting the tool. *Methods:* Conventional and tool-guided manual insertions were performed by expert cochlear implant surgeons in an analog temporal bone model that allows to simultaneously record intracochlear pressure, insertion forces and electrode array deformation. *Results:* Comparison between conventional and tool-guided insertions demonstrate a substantial reduction of maximum insertion forces, force variations, transverse intracochlear electrode array movement, and pressure transients. *Conclusion:* The presented tool can be utilized in manual cochlear implantation and significantly improves key metrics associated with intracochlear trauma. *Significance:* The instrument may ultimately help improve hearing outcomes in cochlear implantation. The versatile design may be used in both manual cochlear implantation and motorized and robotic insertion, as well as image-guided surgery.**

***Index Terms*—Cochlear implant, insertion tool, surgical tool.**

I. Introduction

SCALAR translocation of cochlear implant electrode arrays (EAs) is regularly observed in postsurgical medical imaging [1], and more subtle traumatic events, such as fracture of the osseous spiral lamina, damage to the modiolus and elevation or rupture of the basilar membrane—even if hard to attest in clinical cases—are documented well in cadaveric experiments [2], [3]. These injuries potentially entail the formation of fibrotic tissue and new bone growth, disrupt normal cochlear function by impeding cochlear homeostasis and may ultimately lead to reduced electrical and acoustic hearing performance [4], [5]. With the importance of this surgical step widely recognized, surgical recommendations have been developed that are popularly referred to as the soft-surgery approach [6]. However, aside from these sensible measures for the gentle handling of the EA, little has changed since the early days of cochlear implantation.

In this work, we introduce a concept for improved guiding of an EA in cochlear implantation, based on a removable, redirecting sleeve.

II. Rationale

Insertions parallel to the basal portion of the cochlea cause lower forces and reduce intracochlear trauma [3], [7]. Several image-guided approaches were proposed to indicate optimal trajectories [8], [9], [10], [11]. Unfortunately, parallel access to the scala tympani is rarely possible due to anatomical restrictions posed by the facial nerve and cochlear hook region [12]. Current concepts mainly seek to mitigate intracochlear trauma by passively guiding the array and motorizing the insertion process [13], [14], [15], [16], thereby precluding tremor. There is debate, however, whether complex robotic solutions will gain widespread adoption [17], [18].

Herein, we present a concept for a surgical tool for manual cochlear implant EA insertions. The tool has a curved redirecting sleeve that guides the EA through the round window and protrudes slightly into the cochlear lumen. This enables the insertion trajectory to be optimized beyond anatomical constraints. Our design features two key characteristics that make it potentially atraumatic and easily removable.

First, the sleeve obtains stiffness only through the interaction with an enclosed EA, analogous to an inflatable structure. During placement, the sleeve is empty, allowing it to deform if necessary,

Manuscript received 18 March 2022; revised 14 July 2022; accepted 31 August 2022. Date of publication 5 September 2022; date of current version 20 February 2023. This work was supported by the J&K Wonderland foundation and the Emperor foundation. *(Corresponding author: Philipp Aebischer.)*

Philipp Aebischer is with the Department for Otolaryngology, Head and Neck Surgery, Inselspital University Hospital Bern, 3010 Bern, Switzerland, and also with Hearing Research Laboratory, ARTORG Center for Biomedical Engineering Research, University of Bern, 3012 Bern, Switzerland (e-mail: philipp.aebischer@unibe.ch).

Stefan Weder, Georgios Mantokoudis, and Mattheus Vischer are with the Department for Otolaryngology, Head and Neck Surgery, Inselspital University Hospital Bern, Switzerland.

Marco Caversaccio and Wilhelm Wimmer are with the Department for Otolaryngology, Head and Neck Surgery, Inselspital University Hospital Bern, Switzerland, and also with Hearing Research Laboratory, ARTORG Center for Biomedical Engineering Research, University of Bern, Switzerland.

Digital Object Identifier 10.1109/TBME.2022.3204069

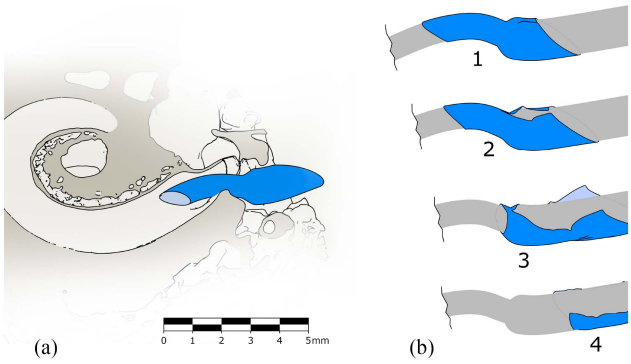

Fig. 1. (a) Cut through the basal plane of a cochlea with the redirecting sleeve (blue) placed. (b) Steps 1–4: After electrode array insertion, the sleeve is removed by retraction, which causes a tear to propagate along its length until it is fully opened.

thus giving way to encountered forces. However, an EA guided through the sleeve displaces the wrinkles, forcing it to adapt to the sleeve's original shape. Since the EA prevents kinking, the sleeve is only subjected to tensile loads, which even very thin plastic films can handle. The potential for redirection thus stems not from inherent stiffness, allowing the empty sleeve to be less stiff than the EA it redirects. This potentially limits intracochlear injury from placing the tool.

Second, the sleeve can easily be retracted with the EA held in place. This is achieved with a small cut in the distal portion (relative to the cochlea) of the sleeve: upon retraction, the cut propagates along the length of the sleeve and the structure opens step by step, until free to be removed. A sequence illustrating this process is shown in Fig. 1.

III. Methods

The aim of the present study is to compare the insertion forces, intracochlear pressure, and insertion mechanics between a newly developed insertion tool and the conventional surgical procedure during the insertion of EAs into a temporal bone model.

Regular insertions, which were performed in the same way as in clinical practice, are hereafter referred to as "conventional," while insertions assisted by the insertion tool are referred to as "tool-guided".

A. Study Protocol

Sixty-six insertions were performed in equal numbers by three expert otologists which regularly conduct cochlear implantations at our institution, and the first author.

Conventional insertions were performed under surgical microscope view (M525, Leica Microsystems GmbH, Wetzlar, Germany), with conventional surgical tools provided. The surgeons were instructed to insert the electrode atraumatically, following the procedure of an implantation with residual hearing according to the soft surgery protocol [19]. They were otherwise free to use their preferred insertion technique.

Tool-guided insertions were undertaken under endoscopic view, using a digital endoscope (MD-V1000LH-120, MISUMI Electronics Corp., New Taipei City, Taiwan) mounted at the superior border of the facial recess. The surgeons received a rundown on the insertion procedure and were provided with the tool correctly installed. No training runs were performed. The implant was grabbed at the extracochlear portion and the guide rail was irrigated, allowing surface tension to cause the EA to adhere. The implant was slowly pushed into the scala tympani, and without releasing the forceps, the magnetic fixation was opened and the electrode guide retracted. Procedural steps of the workflow for both conventional and tool-guided insertions are shown in Fig. 2.

B. Insertion Tool

The insertion tool consists of a *mounting base* (Fig. 3(a)) and an *electrode guide* (Fig. 4). The former is anchored in the mastoidectomy and is used to secure the electrode guide. The electrode guide includes a guide rail and a redirecting sleeve attached to its tip and is used to guide the EA into the cochlea and optimize its path through the cochlear hook region. The assembled tool is shown in Fig. 3(b).

1) Redirecting Sleeve: The sleeve reproduces the thickness profile of the basal part of the EA . The distal portion (with respect to the cochlea) has a diameter of $1.3\,\mathrm{mm}$, and is designed to be placed within the round window niche. The proximal portion has a diameter of $0.8\,\mathrm{mm}$, length of $2.5\,\mathrm{mm}$ and is inserted through the round window. Both ends are curved in opposite directions, resembling an S-shape. While the extracochlear portion is comparably stable, the intracochlear portion is designed as thin as possible, minimizing its potential to traumatize intracochlear structures.

The individual production steps are shown in Fig. 5. First, high-density polyethylene (HD-PE) tubes with a diameter of $1.3\,\mathrm{mm}$ were stretched on a stepped steel blank corresponding to the targeted thickness profile. This steel blank consists of two tubes with a diameter of $1.3\,\mathrm{mm}$ that slide on a central steel rod (diameter $0.8\,\mathrm{mm}$). The HD-PE tubes are clamped onto the outer tubes and stretched outwards. The elongation causes the film to thin out and adapt to the smaller diameter of the central rod. As a wanted side effect, the stretch-induced anisotropic orientation of the polyethylene chains leads to a reduction in tear resistance along the long axis of the sleeve, facilitating the longitudinal propagation of the opening cut. The straight sleeves were sandwiched between an acrylonitrile butadiene styrene (ABS) inner core and heat shrink tubing, heated, and bent to the final shape on a jig. The sleeves were removed from the ABS core, cut to length and glued onto the tip of a guide rail. Lastly, a small cut was made in the distal, thicker portion of the sleeve to start the tearing upon retraction.

A support structure comprising a soft polyvinyl chloride (PVC) tube was inserted into the distal and middle (but not the intracochlear) portion of the redirecting sleeve during the tool placement. This structure prevents a collapse at the location of the cochlear entry and ensures that, after its removal, the EA can pass through.

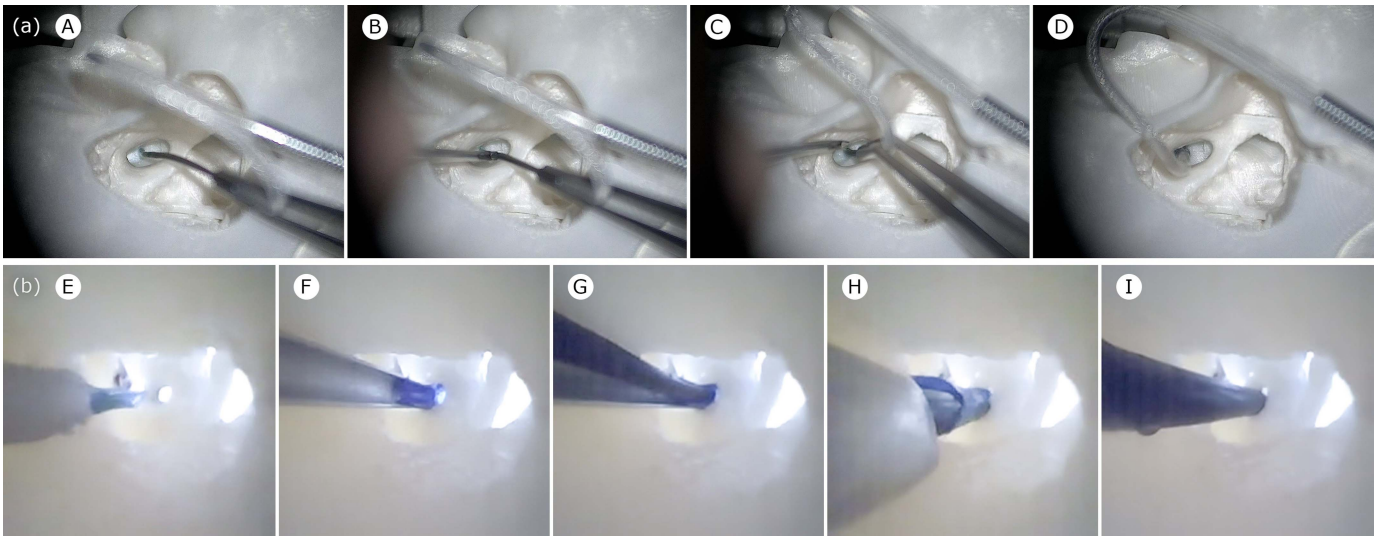

Fig. 2. (a) Surgical microscope view of the mastoidectomy illustrating a conventional insertion. A: Use of forceps to place the electrode array (EA) tip at the round window. B & C: Use of forceps and surgical claw for stabilization of the EA . D: Fully inserted EA . Note that this example is not representative of all insertions, as surgical technique varied among surgeons. (b) Endoscopic view through the facial recess illustrating the usage of the insertion tool: E: Placement of the redirecting sleeve through the round window. F: Electrode guide placed and secured. G: EA is inserted along the guide rail into the cochlea. H: The fully inserted EA is stabilized with forceps near the facial recess and the electrode guide retracted for removal. I: Fully inserted EA with tool removed. Note that the EAs are colored black to improve tracking.

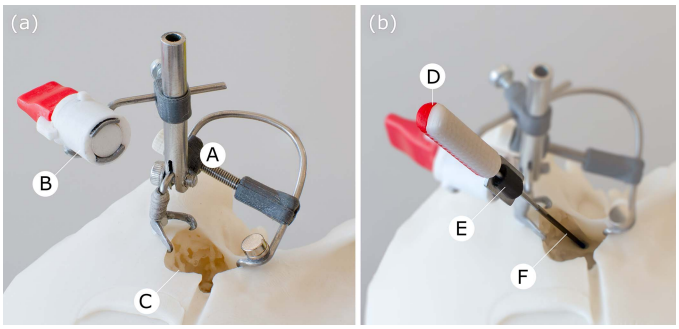

Fig. 3. (a) The mounting base (A) is equipped with a switchable magnet (B) and anchored in the mastoidectomy (C) of the temporal bone model. (b) After placement using the handle (D), the electrode guide is attached to the switchable magnet by a plate (E). A guide rail (F) leads through the facial recess and the tip of the redirecting sleeve is positioned through the round window.

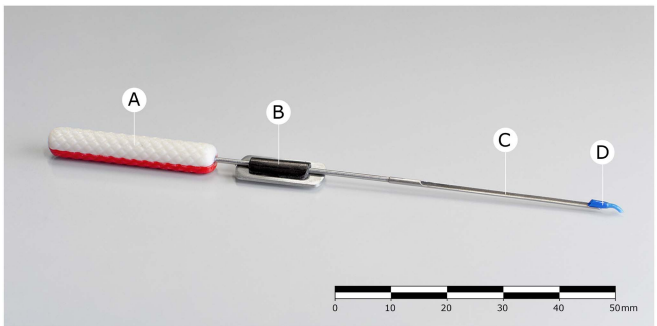

Fig. 4. Prototype of the electrode guide comprised of a grip (A), fixation plate (B), guide rail (C) and redirecting sleeve (D). The electrode guide is secured in place by a mounting base, together forming the insertion tool.

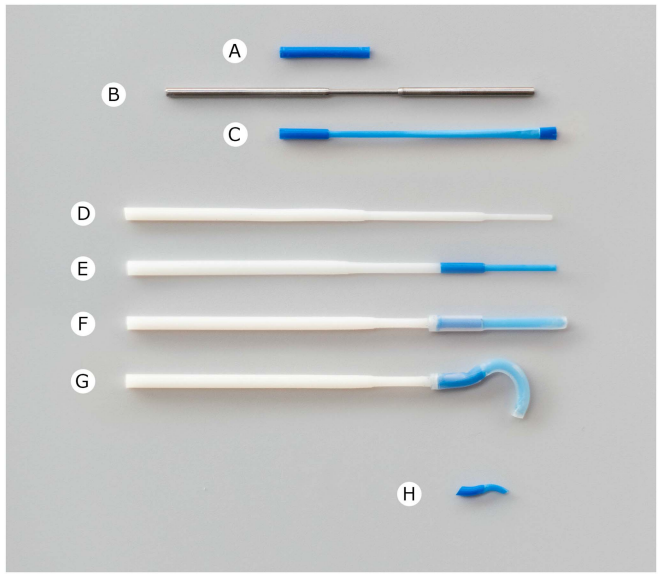

Fig. 5. Production steps of the redirecting sleeve. A HD-PE tube (A) is stretched (C) on a steel blank (B), sandwiched between an acrylonitrile butadiene styrene (ABS) inner core and heat shrink tubing (D, E, F), deformed under heat (G) and cut to length (E).

2) Mounting Base: The redirecting sleeve was connected to a concave guide rail, together forming the *electrode guide*. A photograph of the instrument is shown in Fig. 4. For the present study, the electrode guide was held in place by a mounting base anchored in the mastoidectomy. The mounting base and electrode guide mate through a switchable magnet, which allows to easily attach and release the electrode guide by rotating a lever by 90°. Fig. 3(b) shows the mounting base mounted to the temporal bone model with the electrode guide attached. It

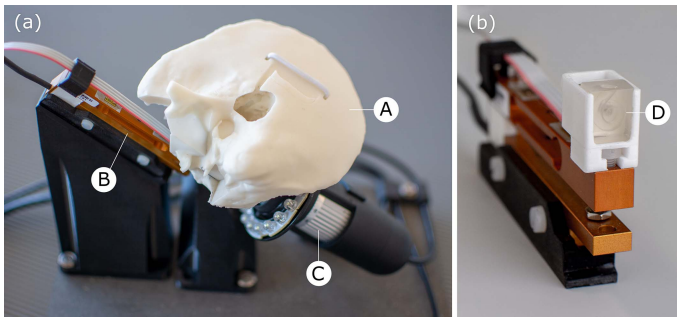

Fig. 6. (a) Measurement setup consisting of a temporal bone model (A) with mastoidectomy and implant bed, load cell (B) measuring force along the direction of insertion and microscope with illumination (C) orthogonal to the basal plane of the cochlea. The orientation of the model corresponds to a regular surgical setting [7]. (b) Extracted load cell with mounted scala tympani model (D). A pressure sensor is positioned at the cochlear apex (hidden behind the model).

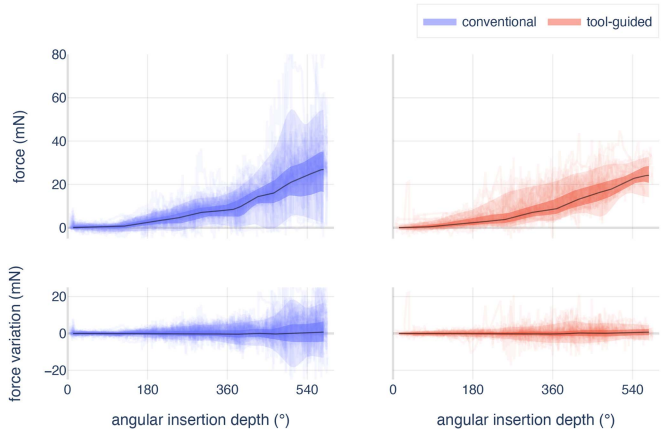

Fig. 7. Force and force variation as running median (solid line), interquartile range (shaded area) and 5th to 95th percentile (lighter area). Left column shows data for conventional insertions, right column tool-guided insertions.

should be noted that many alternative mounting mechanisms are conceivable, and that we did not attempt to evaluate the mounting mechanism in this study.

C. Experimental Setup

1) Temporal Bone Model: A 3D-printed temporal bone model including a mastoidectomy, posterior tympanotomy, cochlear promontory and round window niche was used. The experimental setup is shown in Fig. 6. Within the model, an exchangeable, fully mechanically decoupled scala tympani model is placed to enable the reproducible measurement of insertion forces. The scala tympani model was described previously in full detail [20]. It is a clear epoxy cast of a three-dimensional scala tympani with accurate macro-anatomy obtained from micro computed-tomography images, and reproduces in-vivo frictional properties with use of a hydrophilic polymer brush coating. A thin, flexible film (stretched Parafilm "M" laboratory film, Bemis Compani, Inc, USA) with a punched hole (radius $0.25\,\mathrm{mm}$) was placed at the entrance of the scala tympani model to mimic the soft tissue of the round window membrane. The film was verified to produce no measurable resistance during insertion of the EA and was replaced after each iteration.

2) Cochlear Implant Model: Dummy EAs were glued to the electrode lead of a cochlear implant body (Synchrony, MED-EL GmbH, Innsbruck, Austria). The method for producing the dummy arrays was previously specified [20]. They mirror the geometry and mechanical stiffness of the Flex^{28} electrode array (MED-EL), which was chosen because it is the most implanted type at our institution. In total, sixteen dummy EAs were produced and used in this study, each inserted three to five times.

3) Data Recording and Processing: Data recording and processing in the same experimental setup was also described previously [7]. All measurements were recorded time-synchronously on the same system. Forces were recorded with a load cell (KD78, ME Meßsysteme GmbH, Hennigsdorf, Germany and HX711 load cell amplifier, SparkFun Electronics, Niwot, USA) oriented along the long axis of the scala tympani model, defined by the line within the basal plane of the cochlea connecting the modiolus with the center of the round window. This axis corresponds to the direction of insertion, and allows to capture the majority of the emerging forces [21], [22]. Intracochlear pressure was recorded with a microelectromechanical (MEMS) pressure sensor (MS5837-02BA, Measurement Specialties, Inc; Hampton, USA) attached to the apex of the model. The centerline of the EA was automatically extracted from the video stream of a digital microscope. The angular insertion depth was defined as the azimuth coordinate of the electrode tip and linear insertion depth as the length of the electrode centerline starting at the round window. The insertion work was computed as the integral of the force over the linear insertion depth. Pressure peaks were defined as peaks with a prominence larger than $10\,\mathrm{Pa}$.

IV. Results

A. Insertion Force and Work

The force progression during insertion is shown in the upper row of Fig. 7, grouped by the insertion method. The median insertion forces were similar for the conventional and tool-guided approaches, but there was a tendency for forces to increase more slowly with tool-guided insertion through the apical cochlear turn ($28\,\mathrm{mN}$ per turn compared to $32\,\mathrm{mN}$ per turn).

More prominently, conventional insertions caused significantly higher force variation, in particular during the final phase of the insertion. The corresponding values are shown in the bottom row of Fig. 7. Large variations consequently led to significantly higher maximal forces, with the 95^{th} percentile of observed forces reaching $55\,\mathrm{mN}$ for conventional and $33\,\mathrm{mN}$ for tool-guided insertions.

The distribution of insertion work is shown in Fig. 8. Work is significantly lower for tool-guided insertions (median and interquartile range $119\,\mu\mathrm{J}$ ($94\,\mu\mathrm{J}$ to $170\,\mu\mathrm{J}$) and $152\,\mu\mathrm{J}$ ($125\,\mu\mathrm{J}$ to $176\,\mu\mathrm{J}$), respectively). Three insertions were excluded from the group of tool-guided insertions for this analysis because they did not reach an insertion depth of 495° (the issue

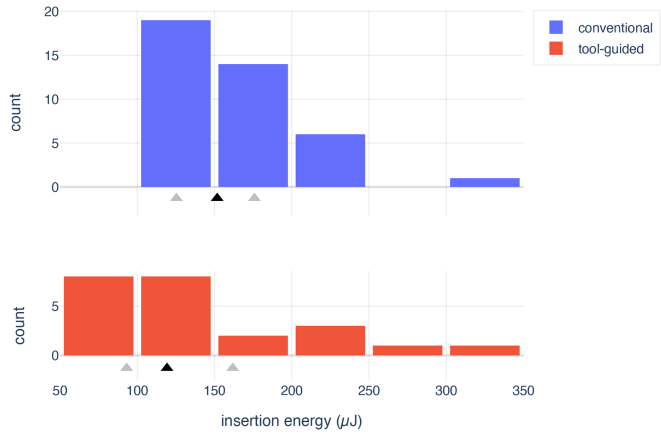

Fig. 8. Insertion work up to an insertion depth of 495°, grouped by the insertion method. Black triangles indicate median values, gray triangles indicate the first and third quartiles. Three insertions not reaching an insertion depth of 495° were excluded from the tool-guided group.

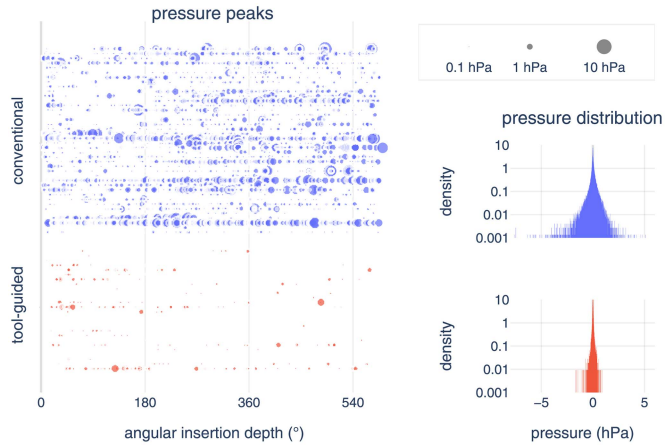

Fig. 10. Left: Pressure peaks as a function of angular insertion depth, grouped by conventional (top) and tool-guided (bottom) insertions. Disk size corresponds to peak height. Right: Histogram showing the distribution of pressure peaks, also grouped by conventional (top) and tool-guided (bottom) insertions.

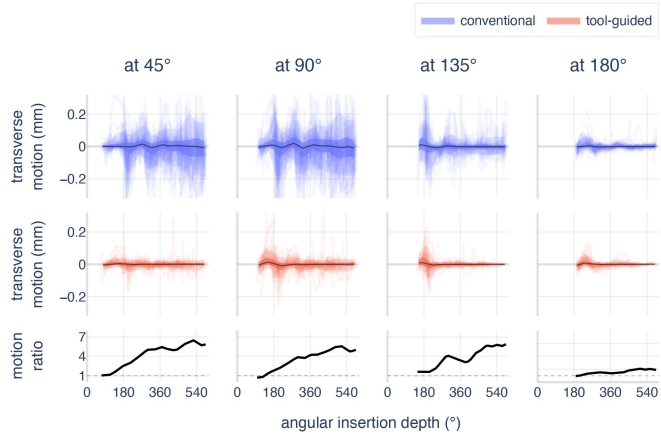

Fig. 9. Transverse EA movement as a function of the angular insertion depth, evaluated at four points in the basal cochlear portion. The data is plotted as running window median (solid line), interquartile range (shaded area) and 5^{th} to 95^{th} percentile (lighter area). The bottom row shows the ratio between median transverse motion of tool-guided and conventional insertions.

of lower insertion depths for some tool-guided insertions is addressed in section Section V-A).

B. Transverse Electrode Movement and Intracochlear Pressure

Tool-guided insertions were accompanied by substantially lower transverse electrode movement inside the first half turn of the scala tympani. The corresponding data is summarized in Fig. 9. During the second stage of the insertion, basal movements were roughly a factor of 6 smaller for the tool-guided insertions compared to the conventional approach.

Furthermore, the tool-guided insertions showed substantially reduced pressure variations. A breakdown of pressure transients is presented in Fig. 10. The pressure peaks in conventional insertions were comparable to values measured in cadaveric implantations [23], while tool-guided insertions showed a reduction of pressure peaks by approximately 29 dB.

C. Tool Retraction

In three cases, the sleeve did not open correctly, leading to retraction of the EA . Except for those failed removals, the EA did not move or slightly increased in insertion depth with an average angular change of $5° \pm 12°$ (mean $\pm$ standard deviation).

Pressure values during the retraction are also included in Fig. 10. Maximal forces occurring upon retraction did not differ significantly from maximal forces during insertion ($p = 0.15$). The same holds true for the observed pressure peaks ($p = 0.08$).

V. Discussion

The insertion tool proved to considerably stabilize the EA during the insertion. This is expressed in a substantial reduction in transverse movement of the EA, consistently accompanied by a substantial reduction in force peak values and intracochlear pressure peaks.

In a regular anatomy, the EA assumes an S-shaped configuration through the hook region of the cochlea. The round window is angled with respect to the basal portion of the scala tympani [22], and consequently, a straight EA will first approximate or even contact the modiolus and subsequently transverse to the lateral wall.

When tremor causes the EA to slightly retract or advance, the movement is not rigidly coupled to the tip because some motion is absorbed through elastic deformation within the S-shaped portion. This causes transverse movement of the EA as well as increased longitudinal forces, which likely are detrimental to the intracochlear structures. Transverse motion can impose additional stress on the modiolus and the first contact point with the lateral wall through constant alteration of applied force and its release. This fits with observations of osseous spiral lamina fractures most often occurring around 25° and injury to the

basilar membrane within the first 180°, where also buckling was observed [13], [22], [24]. Furthermore, the displacement of perilymph may lead to fluid flow that induces local hydraulic trauma and pressure waves that propagate along the cochlea, potentially causing acoustic insult to the hearing organ [25], [26].

Therefore, we hypothesize that reducing intracochlear electrode movement can help to minimize intracochlear trauma. The insertion tool presented here effectively minimizes intracochlear movements and the associated force peaks and pressure transients. The reduction in maximum forces may potentially help to reduce fractures of the osseous spiral lamina and rupturing of the basilar membrane, which is known to occur regularly in cochlear implantation [27], [28].

Encouragingly, the measurements show that retracting the electrode guide does not impose greater loads than the array insertion. Maximal forces and pressure transients upon retraction of the electrode guide were comparable to their corresponding values during insertion, and thus significantly lower than values observed in conventional insertion. In addition, the tool promises a fairly uncomplicated integration into the conventional workflow.

A. Challenges

Two main challenges were identified in this study. First, the extracochlear portion of the redirecting sleeve restrained the view on the EA near the round window. This limited the surgeon's capability to judge whether an EA was fully inserted. This was further aggravated by the low resolution of the digital endoscope. Indeed, we observed that the insertion was often stopped when the stopper reached the extracochlear portion of the redirecting sleeve, about 2 mm short of a full insertion. This translated into lower insertion depths with the insertion tool (average linear depth $24.8\,\mathrm{mm}$ and angular depth 541°, compared to $26.9\,\mathrm{mm}$ and 629° for conventional insertions). It should be noted that this was not a result of a mechanical limitation of the insertion tool, but rather a methodological issue. In general, we suspect that this problem was aggravated by the use of the black colored dummy EAs. With no visible texture, they make it difficult to assess any movement. Several approaches exist to mitigate this problem. The original implants feature a colored marker near to the marker ring that indicates a fully inserted position, which was not present in the dummy EAs. The extracochlear portion of the sleeve could be trimmed such that its edge coincides with the marker at full insertion. Alternatively, the step-up in sleeve diameter could be omitted altogether. In this case, the distal, thicker part of the electrode lead would open the sleeve, leaving the lead visible. Additionally, the sleeve could be made from a transparent material.

Secondly, further testing is required to evaluate the placement of the tool. We anticipated that some training is required for consistently achieving correct placement. Therefore, the procedure was not included in the study protocol to avoid incorrect placement affecting the subsequent EA insertion. During the preparatory placement of the tool, the main focus was thus on correct positioning. While the average forces were overall low (median $4\,\mathrm{mN}$ (interquartile range $-1\,\mathrm{mN}$ to $5\,\mathrm{mN}$)), short force peaks could reach rather high values in some instances (median maximal values $24\,\mathrm{mN}$ ($13\,\mathrm{mN}$ to $36\,\mathrm{mN}$)). We hypothesize that careful placement allows to limit the maximal forces to an acceptable limit, as already observed in several instances (in six cases, the maximal forces were below $10\,\mathrm{mN}$).

Further improvement may be achieved by mechanical changes and process optimization. The final film thickness of the intracochlear portion of the redirecting sleeve was limited by our manual production process. It is likely that a lower film thickness would be beneficial for reducing the forces upon tool placement without adverse impact on other functioning. Additionally, the shape of the sleeve's tip may be optimized and the length of placement support reduced. The sleeve also might be inserted in a collapsed state, making it more compliant.

B. Limitations

The study was carried out in an analog temporal bone model. For the first evaluation of a prototype, this is an adequate choice providing repeatability, intracochlear force measurement and the possibility to optically evaluate the EA position. Further work needs to assess the influence of anatomical variations and the tool's impact on anatomical structures, which might better be studied in cadaver specimen.

Our setup provides force measurement along a single axis. While this is a common measurement configuration that facilitates comparisons with other studies, three-dimensional measurement could provide additional insight into the insertion mechanics [21], [22], [29].

In contrast to the conventional procedure, tool-guided insertions were carried out under endoscopic vision. Surgeon feedback indicated low satisfaction with this mode of visualization because only the distal portion of the electrode guide was displayed within the facial recess, providing no view of the guide rail, forceps, or electrode lead within the mastoidectomy. This may have a negative impact on surgeon dexterity. Future experiments should investigate tool-guided insertions under normal microscopic vision which cochlear implant surgeons are already accustomed to.

Experienced surgeons have been shown to accurately determine the optimal insertion axis to within a few degrees [30]. Tool placement based purely on the surgeon's anatomical expertise may therefore be possible, but this hypothesis remains to be tested. Further guidance could be derived from preoperative computed tomography images, possibly with a visualization through automatic segmentation of anatomical structures [31], augmented reality overlays [32] or customized mastoid templates [10] to indicate optimal tool placement.

VI. Conclusion

We presented a concept for an insertion tool for cochlear implantation that guides the EA through the hook region and achieves a significant reduction of intracochlear force and pressure transients. Owing to its design, it is potentially protective towards the delicate inner ear anatomy and is easily removed after the insertion.

We found that the tool significantly reduces maximal insertion forces and the total energy deposited to the inner ear when compared to conventional insertions in an analog temporal bone model. Furthermore, the stabilization and redirection away from the modiolus helps to drastically decrease transverse movement of the EA and intracochlear pressure peaks.

Potential applications of the proposed design include conventional cochlear implantation, as well as use with image-guided approaches and motorized tools.

REFERENCES

[1] W. G. Morrel et al., "Effect of scala tympani height on insertion depth of straight cochlear implant electrodes," *Otolaryngology–Head Neck Surg.*, vol. 162, no. 5, pp. 718–724, Feb. 2020.

[2] C. G. Wright and P. S. Roland, *Cochlear Anatomy Via Microdissection With Clinical Implications*. Berlin, Germany: Springer, 2018.

[3] R. Torres et al., "Cochlear implant insertion axis into the basal turn: A critical factor in electrode array translocation," *Otol. Neurotol.*, vol. 39, no. 2, pp. 168–176, Feb. 2018.

[4] G. B. Wanna et al., "Impact of intrascalar electrode location, electrode type, and angular insertion depth on residual hearing in cochlear implant patients: Preliminary results," *Otol. Neurotol.*, vol. 36, no. 8, pp. 1343–1348, Sep. 2015.

[5] T. Kamakura and J. B. Nadol, "Correlation between word recognition score and intracochlear new bone and fibrous tissue after cochlear implantation in the human," *Hear. Res.*, vol. 339, pp. 132–141, Sep. 2016.

[6] E. Lehnhardt, "Intracochlear placement of cochlear implant electrodes in soft surgery technique," *HNO*, vol. 41, no. 7, pp. 356–359, 1993.

[7] P. Aebischer et al., "In-vitro study of speed and alignment angle in cochlear implant electrode array insertions," *IEEE Trans. Biomed. Eng.*, vol. 69, no. 1, pp. 129–137, Jan. 2022.

[8] R. Yasin et al., "Investigating variability in cochlear implant electrode array alignment and the potential of visualization guidance," *Int. J. Med. Robot. Comput. Assist. Surg.*, vol. 15, no. 6, Dec. 2019, Art. no. e2009.

[9] D. Bautista-Salinas et al., "Integrated augmented reality feedback for cochlear implant surgery instruments," *IEEE Trans. Med. Robot. Bionics*, vol. 3, no. 1, pp. 261–264, Feb. 2021.

[10] W. G. Morrel et al., "Custom mastoid-fitting templates to improve cochlear implant electrode insertion trajectory," *Int. J. Comput. Assist. Radiol. Surg.*, vol. 15, no. 10, pp. 1713–1718, May 2020.

[11] W. Wimmer et al., "Semiautomatic cochleostomy target and insertion trajectory planning for minimally invasive cochlear implantation," *BioMed Res. Int.*, vol. 2014, pp. 1–8, 2014.

[12] X. Meshik et al., "Optimal cochlear implant insertion vectors," *Otol. Neurotol.*, vol. 31, no. 1, pp. 58–63, Jan. 2010.

[13] C. R. Kaufmann et al., "Evaluation of insertion forces and cochlea trauma following robotics-assisted cochlear implant electrode array insertion," *Otol. Neurotol.*, vol. 41, no. 5, pp. 631–638, Jun. 2020.

[14] R. Torres et al., "Restoration of high frequency auditory perception after robot-assisted or manual cochlear implantation in profoundly deaf adults improves speech recognition," *Front. Surg.*, vol. 8, Sep. 2021, Art. no. 729736.

[15] W. Wimmer et al., "Cone beam and micro-computed tomography validation of manual array insertion for minimally invasive cochlear implantation," *Audiol. Neurotol.*, vol. 19, no. 1, pp. 22–30, 2014.

[16] W. Wimmer et al., "Electrode array insertion for minimally invasive robotic cochlear implantation with a guide tube," *Int. J. Comput. Assist. Radiol. Surg.*, vol. 11, no. S1, pp. 80–81, Jun. 2016.

[17] K. E. Riojas and R. F. Labadie, "Robotic ear surgery," *Otolaryngologic Clin. North Amer.*, vol. 53, no. 6, pp. 1065–1075, Dec. 2020.

[18] M. Caversaccio et al., "Robotic middle ear access for cochlear implantation: First in man," *PLOS ONE*, vol. 14, no. 8, Aug. 2019, Art. no. e0220543.

[19] T. Lenarz, "Cochlear implant state of the art," *Laryngo-Rhino-Otologie*, vol. 96, no. S.1, pp. S123–S151, May 2017.

[20] P. Aebischer, M. Caversaccio, and W. Wimmer, "Fabrication of human anatomy-based scala tympani models with a hydrophilic coating for cochlear implant insertion experiments," *Hear. Res.*, 2021, Art. no. 108205.

[21] J. T. Roland, "A model for cochlear implant electrode insertion and force evaluation: Results with a new electrode design and insertion technique," *Laryngoscope*, vol. 115, no. 8, pp. 1325–1339, Aug. 2005.

[22] E. Avci et al., "Three-dimensional force profile during cochlear implantation depends on individual geometry and insertion trauma," *Ear Hear.*, vol. 38, no. 3, pp. e168–e179, 2017.

[23] R. M. Banakis Hartl and N. T. Greene, "Measurement and mitigation of intracochlear pressure transients during cochlear implant electrode insertion," *Otol. Neurotol.*, vol. 43, no. 2, pp. 174–182, Nov. 2022.

[24] R. Torres et al., "Atraumatic insertion of a cochlear implant pre-curved electrode array by a robot-automated alignment with the coiling direction of the scala tympani," *Audiol. Neurotol.*, vol. 27, no. 2, pp. 148–155, Jul. 2021.

[25] N. T. Greene et al., "Intracochlear pressure transients during cochlear implant electrode insertion," *Otol. Neurotol.*, vol. 37, no. 10, pp. 1541–1548, Dec. 2016.

[26] A. A. Eshraghi and T. R. Van De Water, "Cochlear implantation trauma and noise-induced hearing loss: Apoptosis and therapeutic strategies," *Anat. Rec. Part A: Discoveries Molecular, Cellular, Evol. Biol.*, vol. 288A, no. 4, pp. 473–481, Apr. 2006.

[27] T. Ishii, M. Takayama, and Y. Takahashi, "Mechanical properties of human round window, basilar and reissner's membranes," *Acta Oto-Laryngologica*, vol. 115, no. 519, pp. 78–82, Jan. 1995.

[28] D. Schuster, L. B. Kratchman, and R. F. Labadie, "Characterization of intracochlear rupture forces in fresh human cadaveric cochleae," *Otol. Neurotol.*, vol. 36, no. 4, pp. 657–661, Apr. 2015.

[29] O. Majdani et al., "Force measurement of insertion of cochlear implant electrode arrays in-vitro: Comparison of surgeon to automated insertion tool," *Acta Oto-Laryngologica*, vol. 130, no. 1, pp. 31–36, 2010.

[30] R. Torres et al., "Variability of the mental representation of the cochlear anatomy during cochlear implantation," *Eur. Arch. Oto-Rhino- Laryngol.*, vol. 273, no. 8, pp. 2009–2018, Aug. 2016.

[31] J. Wang et al., "Fully automated segmentation in temporal bone CT with neural network: A preliminary assessment study," *BMC Med. Imag.*, vol. 21, no. 1, Dec. 2021, Art. no. 166.

[32] R. Hussain et al., "Augmented reality for inner ear procedures: Visualization of the cochlear central axis in microscopic videos," *Int. J. Comput. Assist. Radiol. Surg.*, vol. 15, no. 10, pp. 1703–1711, Jul. 2020.